JOURNAL OF AGRICULTURAL AND FOOD CHEMISTRY

Article

pubs.acs.org/JAFC

Metabolomic Analysis and Differential Expression of Anthocyanin Biosynthetic Genes in White- and Red-Flowered Buckwheat Cultivars (*Fagopyrum esculentum*)

Yeon Bok Kim,[†] Soo-Yun Park,[§] Aye Aye Thwe,[†] Jeong Min Seo,[‡] Tastsuro Suzuki,[#] Sun-Ju Kim,[‡] Jae Kwang Kim,*[,⊥] and Sang Un Park*[,†]

[†]Department of Crop Science, Chungnam National University, 99 Daehak-Ro, Yuseong-Gu, Daejeon 305-764, Republic of Korea

[§]Department of Agricultural Biotechnology, National Academy of Agricultural Science (NAAS), 150 Sooin-Ro, Kweonseon-Gu, Suwon 441-707, Republic of Korea

[‡]Department of Bio-Environmental Chemistry, Chungnam National University, 99 Daehak-Ro, Yuseong-Gu, Daejeon 305-764, Republic of Korea

[#]National Agriculture and Food Research Organization, Hokkaido Agricultural Research Center, Sapporo 062-8555, Japan

[⊥]Division of Life Sciences, College of Life Sciences and Bioengineering, Incheon National University, Incheon 406-772, Republic of Korea

Supporting Information

ABSTRACT: Red-flowered buckwheat (*Fagopyrum esculentum*) is used in the production of tea, juice, and alcohols after the detoxification of fagopyrin. In order to investigate the metabolomics and regulatory of anthocyanin production in red-flowered (Gan-Chao) and white-flowered (Tanno) buckwheat cultivars, quantitative real-time RT-PCR (qRT-PCR), gas chromatography time-of-flight mass spectrometry (GC-TOFMS), and high performance liquid chromatography (HPLC) were conducted. The transcriptions of *FePAL*, *FeC4H*, *Fe4CL1*, *FeF3H*, *FeANS*, and *FeDFR* increased gradually from flowering stage 1 and reached their highest peaks at flowering stage 3 in Gan-Chao flower. In total 44 metabolites, 18 amino acids, 15 organic acids, 7 sugars, 3 sugar alcohols, and 1 amine were detected in Gan-Chao flowers. Two anthocyanins, cyanidin 3-*O*-glucoside and cyanidin 3-*O*-rutinoside, were identified in Gan-Chao cultivar. The first component of the partial least-squares to latent structures-discriminate analysis (PLS-DA) indicated that high amounts of phenolic, shikimic, and pyruvic acids were present in Gan-Chao. We suggest that transcriptions of genes involved in anthocyanin biosynthesis, anthocyanin contents, and metabolites have correlation in the red-flowered buckwheat Gan-Chao flowers. Our results may be helpful to understand anthocyanin biosynthesis in red-flowered buckwheat.

KEYWORDS: *anthocyanin, common buckwheat, gene expression, metabolic profiling, red-flowered*

INTRODUCTION

The buckwheat family (Polygonaceae) comprises common buckwheat (*Fagopyrum esculentum*) and tartary buckwheat (*Fagopyrum tataricum*). These two buckwheat species are used as food sources, and one of them is an important alternative crop.[1,2] In addition, they can be grown without the use of chemicals by following sustainable agricultural practices, which involve developing and extending the uses of environmentally conscious technologies. Common buckwheat is cultivated around the world, whereas tartary buckwheat is grown and used in the mountainous regions of southwestern China (Sichuan), northern India, Bhutan, and Nepal. In central European countries, buckwheat has been grown for centuries and is now grown alongside spelt wheat.[3] Tartary buckwheat has yellow-green flowers, wide and short leaves, and jagged seed margins, whereas common buckwheat flowers are generally white, pink, or red. In particular, red-flowered buckwheat is used in the production of tea, juice, and alcohols after the detoxification of fagopyrin.[4] Rutin, which is a bioactive phenolic compound, is industrially important and has antioxidant, anti-inflammatory, antihypertensive, anticarcinogenic, antithrombotic, and vasoconstrictive properties.[5−7] The rutin content of the common buckwheat is the highest in its flowers [6809 mg/100 mg dry weight (DW)] and is 1000 times higher than that in its roots (6.25 mg/100 mg DW).[8] Common buckwheat seeds are used to make many foods, such as pancakes, breads, noodles, and tea. Common buckwheat is a source of vitamins, essential amino acids, and phenolic compounds.[5]

Flavonoids are the largest group of secondary metabolites in plants. They are also classified into flavonols, flavones, flavanones, catechins, anthocyanidins, and chalcones.[9] Phenylpropanoid compounds are synthesized from a variety of enzymes and play important roles such as in pigment production, photoprotection, and disease resistance (Figure 1).[9,10]

The first enzyme of the phenylpropanoid pathway is a phenylalanine ammonia-lyase (PAL), which catalyzes the

Received: May 23, 2013
Revised: September 30, 2013
Accepted: October 1, 2013
Published: October 1, 2013

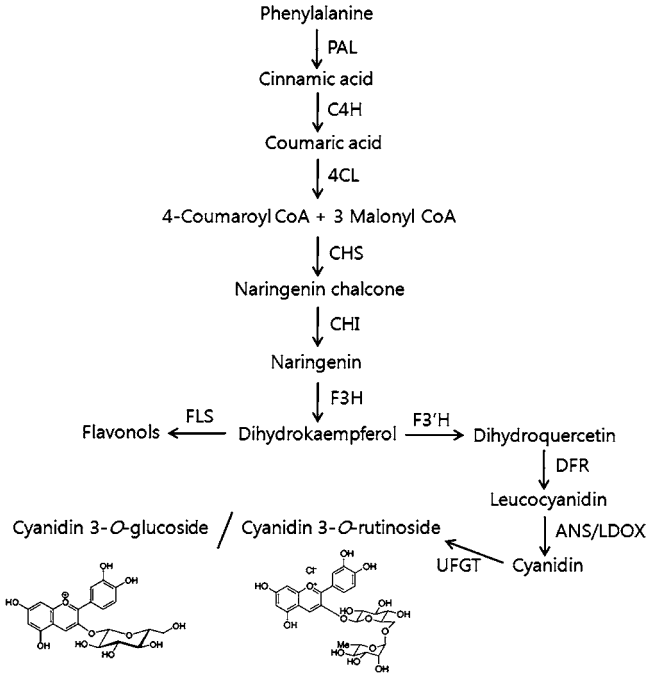

Figure 1. Simplified scheme of the flavonoid pathway in *Fagopyrum esculentum*.[21,26] PAL, phenylalanine ammonia-lyase; C4H, cinnamate 4-hydroxylase; 4CL, 4-coumaroyl CoA ligase; CHS, chalcone synthase; CHI, chalcone isomerase; F3H, flavone 3-hydroxylase; FLS, flavonol synthase; F3′H, flavonoid 3′-hydroxylase; ANS/LDOX, anthocyanidin synthase/leucoanthocyanidin dioxygenase; DFR, dihydroflavonol-4 reductase; UFGT, UDP-flavonoid glucosyl transferase.

conversion of L-phenylalanine into *trans*-cinnamic acid. Following this, cinnamate-4-hydroxylase (C4H), which is the first cytochrome P450-dependent monooxygenase of the phenylpropanoid pathway, catalyzes the hydroxylation of *trans*-cinnamic acid into *p*-coumaric acid.[11] Next, 4-coumarate, which is a coenzyme-A (CoA) ligase (4CL), converts *p*-coumarate into its CoA ester. This product serves as a precursor for various phenylpropanoid biosynthetic derivatives, including lignins and flavonoids. Subsequently, chalcone synthase (CHS) catalyzes the production of a tetrahydroxychalcone by using malonyl CoA and 4-coumaroyl CoA as substrates in the committed step of flavonoid pathway and is highly regulated by the presence of multiple isozymes.[9] Following this, chalcone isomerase (CHI), which catalyzes the conversion of chalcone into naringenin, is converted into dihydrokaempferol and dihydroquercetin by flavone 3-hydroxylase (F3H) and flavonoid 3′-hydroxylase (F3′H), respectively. F3′H acts on the β-ring of dihydrokaempferol to bring about the formation of dihydroquercetin, which is the precursor of all cyanidin pigments. Next, the enzyme dihydroflavonol 4-reductase (DFR) catalyzes the stereospecific reduction of dihydroflavonol into leucoanthocyanidins (flavan-3,4-diol) by using NADPH as a cofactor.[12,13] The dehydration of leucoanthocyanidin by anthocyanidin synthase (ANS) concludes the production of anthocyanidins.[14] The enzymes involved in flavonoid biosynthesis have been extensively studied in maize, petunias, snapdragons, and *Arabidopsis*.[9] Previously, our group reported the expression levels of flavonoid biosynthesis genes and the accumulation of phenolic compounds in common buckwheat and radish.[8,15] Flavonols and flavones are synthesized from a branch of the phenylpropanoid pathway, and they are conjugated into sugars, primarily glucose, rhamnose, and rutinose.[16]

Secondary metabolites are derived from the central or primary metabolic processes in plants. The primary metabolite profile of an organism is closely related to its phenotype and shows the important nutritional characteristics of the organism.[17,18] Thus, primary core metabolites permit good metabolite discrimination between genotypes or mutants. However, metabolomics generate complex data tables that are hard to summarize and interpret without appropriate statistical and visualization tools. Multivariate statistical methods, such as principal component analysis (PCA), partial least-squares to latent structures (PLS), and orthogonal PLS (OPLS), reduce the dimensionality of complex data sets, facilitating the visualization of inherent patterns in the data.[19]

In this study, hydrophilic metabolic profiling of two cultivars' flowers was carried out by using gas chromatography time-of-flight mass spectrometry (GC-TOFMS) coupled with chemometrics to determine their phenotypic variations. Additionally, we compared the expressions of anthocyanin biosynthetic genes in different organs of two buckwheat cultivars. Finally, anthocyanins from different organs were analyzed using high-performance liquid chromatography (HPLC).

MATERIALS AND METHODS

Chemicals and Solvents. For the chemical analysis of anthocyanins, the external standard cyanidin 3-*O*-glucoside chloride was purchased from Fujicco Co., Ltd. (Kobe, Japan). HPLC-grade acetonitrile (CH_3CN) was purchased from J. T. Baker Chemical Co. (Phillipsburg, NJ, USA), and formic acid was provided by Kanto Chemical Co., Inc. (Tokyo, Japan).

Preparation of Plant Materials. Two cultivars of common buckwheat, the red-flowered Chinese variety (Gan-Chao) and the white-flowered (Tanno) variety, were bred by the National Agricultural Research Center (Hokkaido, Japan). For biological replications, seeds were sown in 12 pots (total 24 plants) filled with perlite-mixed soil in the Chungnam National University greenhouse (Daejeon, Korea) on May 10, 2012; two seeds were sown in one pot. To investigate the accumulation pattern of anthocyanin, white and red petals were classified for each growth stage and harvested. According to the method of Suzuki et al.,[20] we chose three flowering stages: stage 1, 0.4−0.8 mg fresh weight (FW); stage 2, 1.6−2.6 mg FW; and stage 3 (fully developed petals), 2.6−3.6 mg FW. Different organs (seed stages 1 and 2; flower stages 1, 2, and 3; stems; young leaves; old leaves; and roots) were harvested 6 weeks after sowing, frozen in liquid nitrogen, and stored at −80 °C until use. Each sample was used for quantitative real-time RT-PCR (qRT-PCR), anthocyanin analysis, and metabolic profiling.

Total RNA Extraction and qRT-PCR Analysis. Two different methods were used to extract the total RNA. Total RNA from the sprouts was isolated by using an Easy BLUE Total RNA Kit (iNtRON, Korea). For assessing complex polysaccharides, each type of organ was subjected to extraction by using a slightly modified cetyltrimethylammonium bromide (CTAB) method.[21] The quantity of RNA was assessed by using a NanoVue Plus spectrophotometer (GE Health Care Life Sciences, USA), and its quality was confirmed by running 1 μg of the RNA on a 1.2% formaldehyde RNA agarose gel. Then, 1 μg of total RNA was reverse-transcribed by using a ReverTra Ace-α (Toyobo, Osaka, Japan) Kit and oligo $(dT)_{20}$ primers according to the manufacturer's protocol. Gene-specific primers were designed for qRT-PCR as described previously by our group.[8] The histone *H3* gene (GenBank accession no. HM628903) was used as a reference gene because of its stable transcript level in each organ. A SYBR Green qRT-PCR assay was performed on a total volume of 20 μL that contained 10 μL of 2× SYBR Green Real-time PCR master mix (Toyobo, Osaka, Japan), 0.5 μM (each) of specific primers, and template cDNA that had been diluted 20-fold. The amplification

program consisted of 1 cycle at 95 °C for 3 min, which was followed by 40 cycles at 95 °C for 15 s, and then a final cycle at 72 °C for 20 s. Each reaction was performed in triplicate on a CFX96 Real-Time PCR System (Bio-Rad, Hercules, CA, USA) with SYBR Green Real-time PCR Master Mix (Toyobo).

Extraction and Quantification of Anthocyanins. HPLC analysis of the anthocyanins was performed according to the method of Park et al.[15] with slight modifications. Briefly, individual anthocyanins of different buckwheat organs (100 mg of powder) were extracted with ultrapure water that contained 5% formic acid (v/v) by vortexing for 5 min and sonicating at room temperature for 20 min under weak light. Following this, the crude extract was centrifuged at 12000 rpm at 4 °C for 15 min. The supernatant was filtered through a 0.45 μm PTFE syringe filter (⌀ 13 mm) for HPLC analysis. The anthocyanin filtrate was analyzed using a Perkin-Elmer Flexar HPLC system (Shelton, CT, USA) equipped with a PDA LC detector. The separation of individual anthocyanins was carried out by using a reversed-phase C-18 column [Synergi 4 μ Polar-RP 80A column (250 × 4.6 mm; i.d.; particle size, 4 μm)] equipped with a Security Guard Cartridge Kit AQ C-18 column (4 × 3 mm; i.d.; Phenomenex, Torrance, CA, USA) by employing gradient elution with (A) water/formic acid (95:5, v/v) and (B) acetonitrile/formic acid (95:5, v/v).

The gradient program entailed employing a linear gradient from 5 to 15% solvent B over 35 min[21] as follows: 0−8 min, 5−10%; 8−13 min, 10−13%; 13−15 min, constant at 13%; 15−18 min, 13−15%; 18−25 min, constant at 15%; sudden drop to 5% at 25.1 min; and then at 5% for 10 min. The detection wavelength and column oven temperature were set at 520 nm and 40 °C, respectively. The flow rate was 1.0 mL/min, and the sample injection volume was 10 μL. The quantification of anthocyanins was calculated using an authentic standard (cyanidin-3-*O*-glucoside) by comparing the HPLC peak area, and the results were expressed in milligrams per gram DW.

Metabolic Profiling of the Petals of the Two Cultivars. Polar metabolite extraction was performed as described previously.[23] Twenty milligrams of powdered sample was extracted using 1 mL of 2.5:1:1 v/v/v methanol/water/chloroform. Ribitol (60 μL, 0.2 mg/mL) was added as an internal standard (IS). Extraction was performed at 37 °C with a mixing frequency of 1200 rpm for 30 min by using a Thermomixer Comfort (model 5355, Eppendorf AG, Hamburg, Germany). The solutions were then centrifuged at 16000*g* for 3 min. The polar phase (0.8 mL) was transferred into a new tube, 0.4 mL of water was added to it, and the solution was centrifuged at 16000*g* for 3 min. The methanol/water phase that contained hydrophilic metabolites was dried in a centrifugal concentrator (CVE-2000, Eyela, Japan) for 2 h followed by drying in a freeze-dryer for 16 h. For GC-TOFMS analysis, two-stage chemical derivatization was performed on the extracted metabolites. First, oximation was carried out by dissolving the samples in methoxyamine hydrochloride (20 mg/mL, 80 μL) and incubating them at 30 °C for 90 min. Then, trimethylsilyl (TMS) etherification was performed by adding 80 μL of *N*-methyl-*N*-(TMS)-trifluoroacetamide (MSTFA) at 37 °C for 30 min. GC-TOFMS was performed by using an Agilent 7890A gas chromatograph (Agilent, Atlanta, GA, USA) that was coupled to a Pegasus HT TOF mass spectrometer (LECO, St. Joseph, MI, USA). Each derivatized sample (1 μL) was separated on a 30 mm × 0.25 mm i.d. fused-silica capillary column that was coated with 0.25 μm of CP-SIL 8 CB low-bleed stationary phase (Varian Inc., Palo Alto, CA, USA). The helium gas flow rate through the column was 1.0 mL/min. The split ratio was set at 1:25, and the injector temperature was 230 °C. The temperatures set were as follows: initial temperature of 80 °C for 2 min, followed by an increase to 320 °C at 15 °C/min, and then a 10 min hold at 320 °C. The transfer line and ion source temperatures were 250 and 200 °C, respectively. The scanned mass range was m/z 85−600, and the detector voltage was set at 1700 V.

Statistical Analysis. The data were analyzed by application of Tukey's multiple-range test at $p \leq 0.05$, using SPSS statistical software (version 11.5 for Windows, SPPS Inc., Chicago, IL, USA). All data are given as the mean and standard deviation of triplicate experiments. The quantification of hydrophilic metabolites was performed by using selected ions (Supporting Information Supplemental Table S1). Quantitative calculations of all analytes were based on the peak area ratios relative to that of the IS. The relative quantification data that were acquired from GC-TOFMS were subjected to PLS discriminate analysis (PLS-DA) (SIMCA-P version 12.0; Umetrics, Umeå, Sweden) to evaluate the relationships in terms of similarity or dissimilarity among groups of multivariate data. The PLS-DA output consisted of score plots to visualize the contrast between different samples and loading plots to explain the cluster separation. The data file was scaled using unit variance scaling before all of the variables were subjected to the PLS-DA. In the model, R^2X is the cumulative variation in the X matrix, R^2Y is the cumulative variation in the Y matrix, and Q^2Y is the prediction ability of the Y variable or matrix according to cross-validation.

RESULTS AND DISCUSSION

Phenotypic Characterization of Red- and White-Flowered Buckwheat. To study the regulation of anthocyanin biosynthesis in red-flowered buckwheat, a cultivar of red-flowered buckwheat and a cultivar of white-flowered buckwheat were selected. As shown in Figure 2, Gan-Chao showed red buds, petals, and seeds at stage 1, whereas Tanno showed white buds, petals, and seeds at stage 1. In addition, the stigma and stamen of Gan-Chao were red, whereas those of Tanno were yellow. The sizes of the Tanno flowers and seeds were bigger than those of Gan-Chao. The Gan-Chao stem showed a red color at about 3 weeks after sowing, whereas that of Tanno was green. In the two cultivars, the leaves and roots displayed almost the same colors (data not shown). Zhang and colleagues[24] observed that the pigmentation in kale purple cultivar is highly dependent on low-temperature stress from 12 to 3 °C. Gan-Chao also might display increased reddishness at low temperatures similar to that by purple kale. We plan to examine buckwheat responses to environmental stress in a future study.

Figure 2. Picture of buckwheat flowers and seeds at different growth stages. (A) and (B) show Gan-Chao and Tanno, respectively. F1, F2, and F3 indicate the flowering stages, and SD1 and SD2 indicate the seed stages. The bar size is 10 mm.

Expression of Anthocyanin Biosynthetic Genes. To better understand the mechanisms that control anthocyanin biosynthesis in *F. esculentum*, the transcript levels of anthocyanin regulatory genes were examined in the different organs of Tanno and Gan-Chao. The transcript levels of anthocyanin upstream pathway genes (*FePAL*, *FeC4H*, *Fe4CL1*, and *Fe4CL2*) and anthocyanin biosynthetic genes (*FeCHS*, *FeCHI*, *FeF3H*, *FeF3′H*, *FeFLS1*, *FeFLS2*, *FeANS*, and *FeDFR*) are shown in Figure 3. Genes that encode enzymes of the anthocyanin pathway are classically divided into two groups: early biosynthetic genes and late biosynthetic genes, which display independent activation mechanisms in dicotyledonous

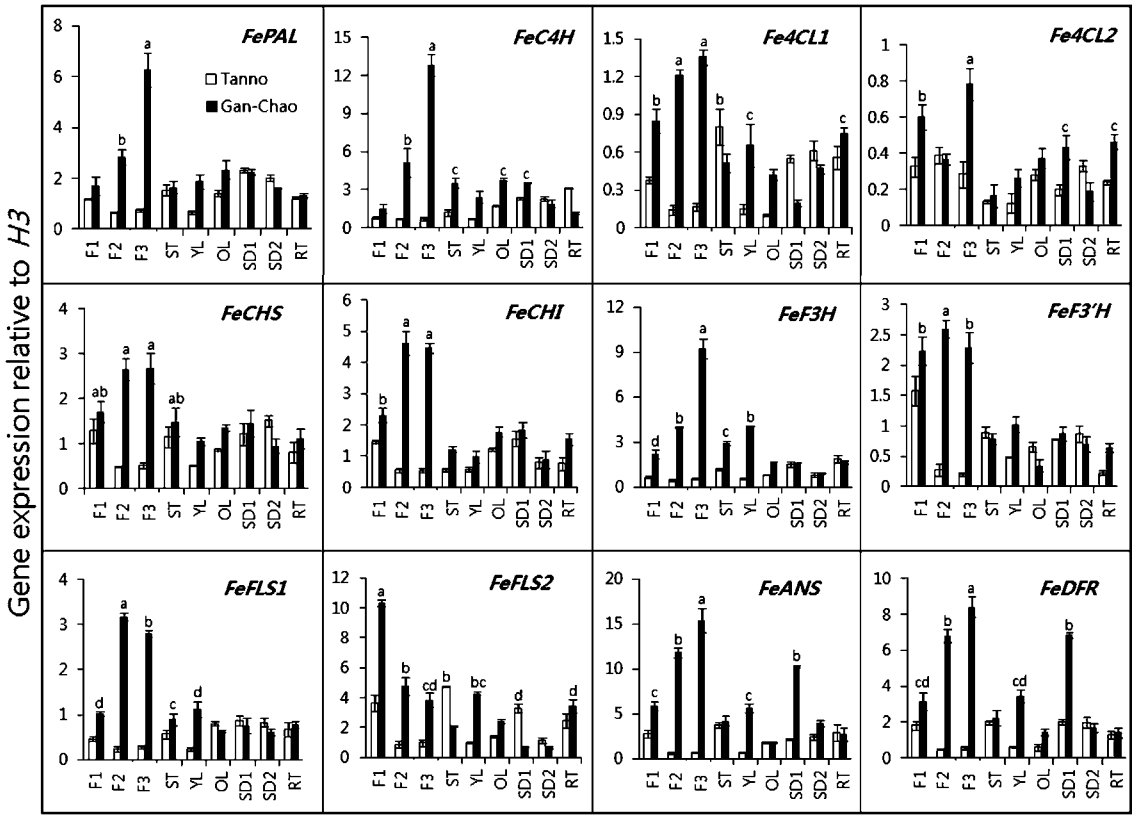

Figure 3. Transcript levels of anthocyanin biosynthesis genes in different organs of Gan-Chao and Tanno. The expression level of each gene is relative to that of the constitutively expressed histone *H3* gene. Each value is the mean of three replicates ± standard deviation (SD).

species.[25,26] Park et al.[27] cloned six genes (*FtC4H*, *Ft4CL*, *FtCHI*, *FtF3H*, *FtF3′H*, and *FtANS*) involved in anthocyanin biosynthesis and described their differential expression in tartary buckwheat. In addition, more recent study by Li et al.[22] described *FtPAL*, *Ft4CL*, *FtF3H*, *FtDFR*, and *FtANS* as being among the main flavonoid biosynthesis pathway genes that showed higher transcript levels compared to the housekeeping gene (histone H3) during the development of tartary buckwheat sprouts. The transcript levels varied widely between the cultivars. The transcript levels of Gan-Chao were much higher than those of Tanno for most of the genes. At the flowering stages, the expressions of genes involved in the anthocyanin biosynthetic pathway dramatically increased in the Gan-Chao cultivar. The transcriptions of *FePAL*, *FeC4H*, *Fe4CL1*, *FeF3H*, *FeANS*, and *FeDFR* increased gradually from flowering stage 1 and reached their highest peaks at flowering stage 3 in the Gan-Chao flower. A reverse scenario was observed for the transcript levels in Tanno, whereby a higher transcript level was observed in flowering stage 1 than in flowering stages 2 and 3 for most of the genes. In the stems of the Hokkai T10 cultivar (stem color: red) of tartary buckwheat, the expressions of all genes involved in anthocyanin biosynthesis, except for *FtF3H*, were higher than those of the Hokkai T8 cultivar (stem color: green).[27] In particular, the transcriptions of *FtPAL* and *FtANS* of the Hokkai T10 cultivar in the stem were about 5-fold higher compared with those of the Hokkai T8 cultivar.[27] Li et al.[8] reported that the expressions in the stem and roots were the highest and that the transcription of *FePAL* in the stem and roots was higher than that in the flowers and leaves. However, in this study, the transcript level of *FePAL* in Tanno was the highest in unripe seeds. In Tanno, only the transcriptions of *Fe4CL1*, *FeFLS2*, and *FeANS* were the highest in stems, whereas *FeF3′H* showed the highest transcription in flowering stage 1.

Only *FeFLS2* was reduced gradually from flowering stages 1 to 3 in Gan-Chao, unlike that of other genes. The transcript level of *FeANS*, which is strongly involved in anthocyanin biosynthesis, was the highest. In addition, the transcriptions of *FeANS* and *FeDFR* in Gan-Chao seeds at stage 1 were 5.7- and 4.9-fold, respectively, which were higher than those of old leaves. Gan-Chao flowering stage 3 exhibited the highest expression level for all genes except *FeCHI*, *FeF3′H*, *FeFLS1*, and *FeFLS2*. Although Tanno had white flowers, low expression levels of all genes involved in anthocyanin biosynthesis were observed (Figure 3). These results show that the up-regulation of *FePAL*, *FeC4H*, *Fe4CL1*, and *Fe4CL2* expressions as well as those of the anthocyanin biosynthetic genes *FeCHS*, *FeCHI*, *FeF3H*, *FeF3′H*, *FeANS*, and *FeDFR* are strongly associated with the high intensity of anthocyanin production in red-flowered buckwheat. Park and colleagues[27] described that the *ANS* genes of two tartary buckwheat cultivars, Hokkai T8 and T10, are more highly expressed than those by the other genes during flowering and seed maturation. Our results were in accordance with their study results. Consequently, we suggest that ANS is an important enzyme with respect to the anthocyanin biosynthesis in tartary and common buckwheat species. Zhang et al.[24] showed that the genes *DFR* and *ANS* in purple kale are rarely expressed in the white cultivar, whereas their transcription levels are high in the purple cultivar. Additionally, Povero et al.[28] suggested that anthocyanin metabolism in tomatoes may be closely interconnected with other important physiological processes and that the tomato

Table 1. Anthocyanin Contents in Gan-Chao and Tanno

cultivar	organ	cyanidin 3-*O*-glucoside[a] (mg/g DW)	cyanidin 3-*O*-rutinoside[a] (mg/g DW)	total[a] (mg/g DW)
Tanno	seed stage1	0.01 ± 0.00 a	ND[b]	0.01 ± 0.00 a
	seed stage 2	ND	ND	ND
	young leaf	ND	ND	ND
	old leaf	ND	ND	ND
	stem	0.01 ± 0.00 a	ND	0.01 ± 0.00 a
	root	ND	ND	ND
	flower stage 1	ND	ND	ND
	flower stage 2	ND	ND	ND
	flower stage 3	ND	ND	ND
red flower	seed stage1	0.02 ± 0.00 b	0.01 ± 0.00 d	0.02 ± 0.00 d
	seed stage 2	ND	ND	ND
	young leaf	ND	0.01 ± 0.00 d	0.01 ± 0.00 d
	old leaf	ND	0.01 ± 0.00 d	0.01 ± 0.00 d
	stem	0.25 ± 0.00 a	0.25 ± 0.02 a	0.50 ± 0.03 a
	root	ND	ND	ND
	flower stage 1	ND	0.02 ± 0.00 d	0.02 ± 0.00 d
	flower stage 2	0.02 ± 0.00 b	0.13 ± 0.00 c	0.15 ± 0.00 c
	flower stage 3	0.02 ± 0.01 b	0.17 ± 0.01 b	0.19 ± 0.01 b

[a]Within each column, values followed by the same letters are not significantly different at $P \leq 0.05$, using Tukey's multiple-range test ($n = 3$). [b]ND, not detected.

genotype may directly or indirectly result in a more general transcriptional reprogramming of genes involved in different metabolic pathways. Anthocyanin synthesis in petunia petals and anthers is regulated by two different ternary MYB−bHLH (basic helix−loop−helix)−WD40 transcription factors. They are composed of the WD40 AN11 and bHLH AN1 proteins, which interact with the R2R3-MYB AN2 proteins in the petals or the R2R3-MYB AN4 in the anthers.[26,29] The expressions of flavonoid biosynthesis regulatory genes appear to be highly dependent on the tissue type or the specific response to internal or external stimuli such as hormones, light, microbial elicitors, UV radiation, sugars, phosphate limitation, or cold stress. This in turn affects signal transduction and the expressions of genes that are involved in the biosynthesis.[30]

Composition of Anthocyanins in Different Organs of Gan-Chao and Tanno Cultivars. Two anthocyanins, cyanidin 3-*O*-glucoside and cyanidin 3-*O*-rutinoside, were identified in different organs of the red-flowered and white-flowered cultivars by HPLC (Table 1). The highest levels of cyanidin 3-*O*-glucoside and cyanidin 3-*O*-rutinoside were found in the stems of Gan-Chao. Inoue et al.[31] reported that cyanidin 3-glucoside, cyanidin 3-galactoside, and cyanidin 3-rhamnosyl galactoside in the hypocotyls of common buckwheat were detected. In addition, Troyer[32] characterized the anthocyanins in buckwheat hypocotyls as derivatives and found that biosynthesis of anthocyanins in *F. sagittatum* depends on light intensity.[33] The anthocyanin contents in different organs of Gan-Chao ranged from 0 to 0.17 mg/g DW, whereas in Tanno they ranged from 0 to 0.01 mg/g DW. In Gan-Chao flowers, the cyanidin 3-*O*-rutinoside content increased gradually from flowering stage 1 (0.02 mg/g DW) to flowering stage 3 (0.17 mg/g DW), whereas cyanidin 3-*O*-glucoside was not detected in flowering stage 1 and was the same in stages 2 and 3 (0.02 mg/g DW). In Gan-Chao, the cyanidin 3-*O*-rutinoside contents of flowering stages 2 and 3 were 6.5- and 8.5-fold, respectively, which were higher than that of flowering stage 1. In comparison with cited reference reported by Suzuki et al.,[20] the red flower of Gan-Chao contained the higher amount of cyanidin 3-*O*-rutinoside (0.03 mg/g DW) than Tanno (0.01 mg/g DW). During flower development of Gan-Chao, cyanidin 3-*O*-rutinoside content at different growth stages of the flower ranged from 0.00006 to 0.003 mg/DW, and stage 5 was the highest.[20] Therefore, in flowering stage 3 of Gan-Chao, total anthocyanins were higher than other tissues. According to these results, flowers of Gan-Chao are expected to be a new anthocyanin-rich material for food processing.

In Tanno, cyanidin 3-*O*-glucoside was detected only in seed stage 1 (0.01 mg/g DW) and in the stem (0.01 mg/g DW). In addition, cyanidin 3-*O*-rutinoside was not detected in any organ. In Gan-Chao, the stem contained 56% of the total anthocyanin content, followed by flowering stages 3 (21.3%), 2 (16.9%), 1 (2.2%), and other organs (1.1%). The anthocyanin content of stem and transcript level of genes involved in anthocynin biosynthesis were not matched. Although the anthocyanin content of Gan-Chao was higher than that of Tanno, the levels greatly varied across organs in both flower types (Table 1). The flavonoid pathway leading to the production of anthocyanins can be divided into two parts. Conversion of 4-coumaroyl-CoA in the flavonoid pathway results in the production of a range of flavonoid compounds, the most common being anthocyanins, proanthocyanidins, aurones, flavones, flavonols, and isoflavonoids.

The major anthocyanin of Gan-Chao is cyanidin 3-*O*-rutinoside, which is widely found in berries[34] and blood oranges,[35] and the next one is cyanidin 3-*O*-glucoside. Cyanidin 3-*O*-glucoside is the major anthocyanin in black soybean seed coats.[36] This may be due to the greater level of anthocyanin pigment accumulation in Gan-Chao than Tanno. Our results were accordance with those of a previously published study.[20] Detection of anthocyanin in Gan-Chao flowers is tightly associated with higher gene expression of *FeCHS*, *FeCHI*, *FeF3H*, *FeF3′H*, *FeANS*, and *FeDFR* in the flavonoid biosynthesis pathway. Suzuki et al.[20] suggested that the anthocyanins, which we identified in buckwheat petals, might have inhibitory effects on the migration of human lung cancer cell lines. In addition, cyanidin distributed in the form of anthocyanins or proanthocyanidin may be an important factor in determining the flower colors.

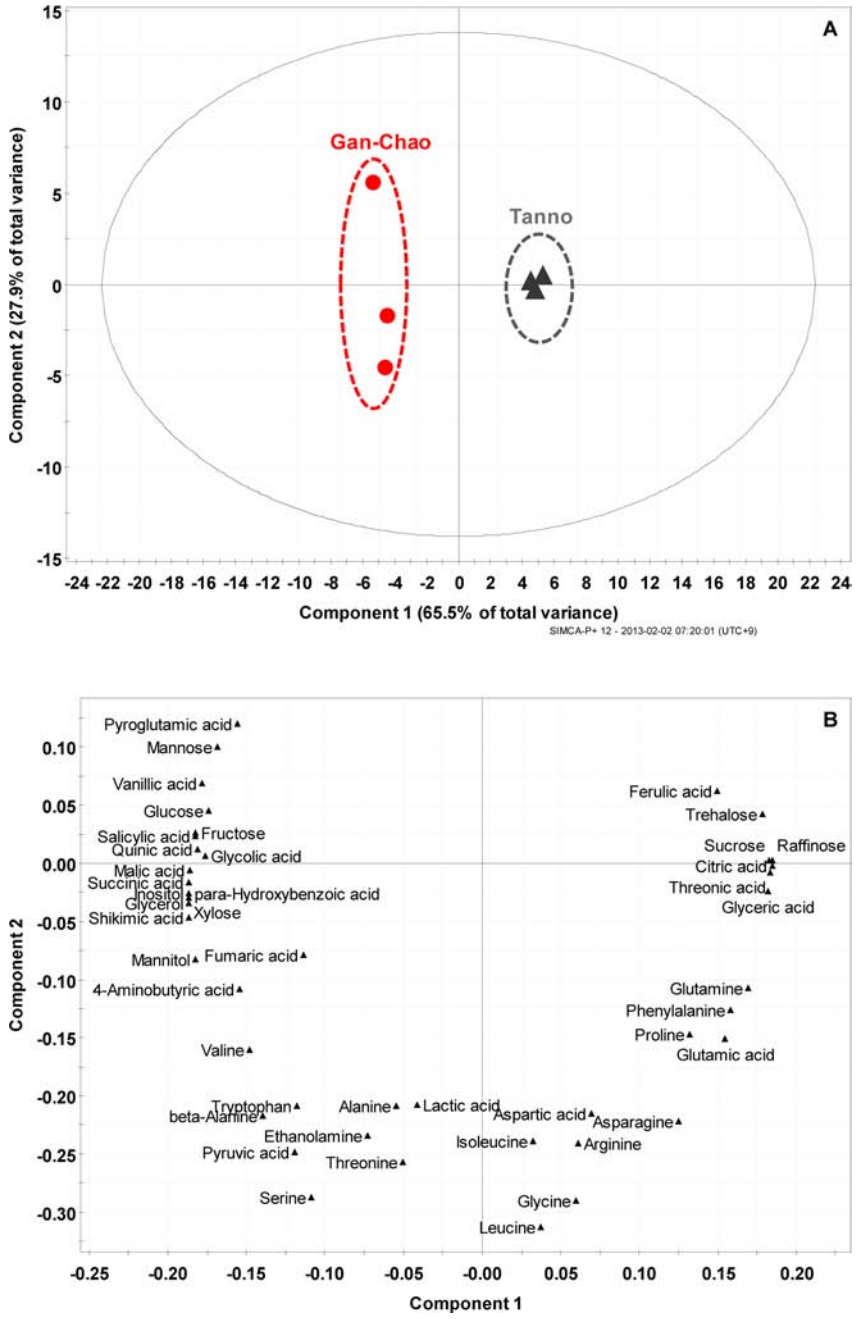

Figure 4. Score (A) and loading (B) plots of principal components 1 and 2 of the partial least-squares discriminant analysis results obtained from polar metabolite data on Gan-Chao and Tanno.

GC-TOFMS Analysis of Polar Metabolites. GC-MS is one of the most popular metabolomic techniques, because it can be used to determine the levels of hydrophilic primary metabolites such as amino acids, organic acids, and sugars through their chemical derivatization. Therefore, GC-TOFMS was used to identify and measure the low-molecular-weight hydrophilic compounds in the buckwheat samples. Chroma-TOF software was used to support peak finding prior to quantitative analysis and for the automated deconvolution of reference mass spectra. The NIST library and an in-house library of spectra obtained using standard chemicals were utilized for compound identification. In total, 44 metabolites, including 18 amino acids, 15 organic acids, 7 sugars, 3 sugar alcohols, and 1 amine, were detected in the Gan-Chao flower (Supporting Information Supplemental Table S1). Very recently, our group detected 47 metabolites, including 19 amino acids, 17 organic acids, 8 sugars, 2 sugar alcohols, and 1 amine, in tartary buckwheat (Hokkai T10) red-colored hairy roots.[37] The corresponding retention times and their fragment patterns are illustrated in Supplemental Table S1 of the Supporting Information. Among the detected metabolites, four phenolic acids (ferulic, *p*-hydroxybenzoic, salicylic, and vanillic acids) were identified. Thwe and Kim et al.[37] identified five phenolic acids (ferulic, *p*-hydroxybenzoic, salicylic, vanillic, and syringic acids) in Hokkai T10 red-colored hairy root were identified.

The GC-TOFMS data were analyzed using a multivariate statistical method to pinpoint the putative metabolites related

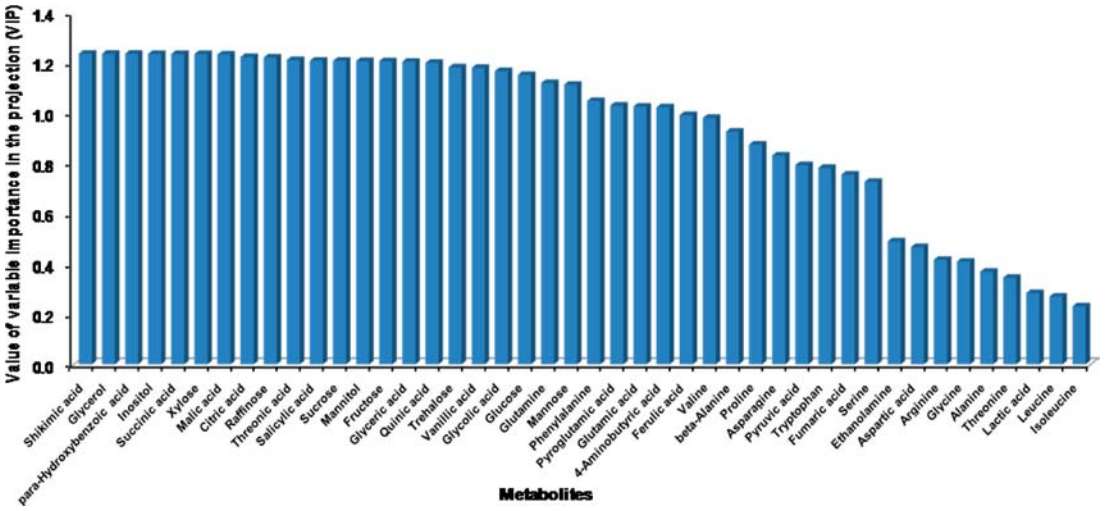

Figure 5. Influence of variables in creating a sample classification for buckwheat flowers.

to genetic variation. The PLS-DA model illustrated a clear separation between the two groups (Figure 4). Identification of the first component aided in resolving the measured composition profiles of the red- and white-flowered cultivars. In the first component of the PLS-DA, the variation was mostly attributable to shikimic acid, for which the eigenvector was −0.1868. In terms of the composition of the genetic varieties, these results suggest that Gan-Chao contains high levels of shikimic acid, inositol, glycerol, xylose, *p*-hydroxybenzoic acid, malic acid, and succinic acid, whereas Tanno contains high levels of raffinose, citric acid, threonic acid, sucrose, and glyceric acid (Supporting Information Supplemental Table S2). Shikimic acid is one of the important building blocks employed in the biosynthesis of phenylpropanoids and is produced from a combination of phosphoenolpyruvate, a glycolytic pathway intermediate, and erythrose 4-phosphate from the pentose phosphate pathway.[37] In a previous study, *β*-alanine, GABA, and succinic acid levels were elevated in *Agastache rugosa* cells, and they induced the accumulation of transcripts of phenylpropanoid genes after exposure to methyl jasmonate.[38] In this study, the metabolites were higher in Gan-Chao than in Tanno.

The PLS-DA model (R^2X = 0.934, R^2Y = 0.997, and Q^2 = 0.981; explaining 99.7% and predictiing 98.1% of the variation in the metabolome data) was generated. For $Q^2 > 0.9$, the model is considered to show excellent predictive ability. The contribution of variables in the projection could be explained using variables important in the projection (VIP). VIP is a weighted sum of squares of the PLS weight, and a value >1 is generally used as a criterion to identify the important variables to the model.[38] In the result of GC-TOFMS analysis, 26 metabolite components had a significant VIP value (>1), as seen in Figure 5. Shikimic acid was the most important for creating a prediction for buckwheat classification (Figure 5). The levels of shikimic acid were 1.3-fold higher in Gan-Chao than in Tanno ($P < 0.001$). The shikimate pathway results in aromatic amino acid metabolism and initiation of the phenylpropanoid pathway. The production of secondary metabolites is tightly related to primary metabolism pathways. Our results indicate that transcriptions of genes involved in anthocyanin biosynthesis, anthocyanin contents, and metabolites have correlation in the red-flowered buckwheat Gan-Chao flowers.

In conclusion, the red-flowered buckwheat Gan-Chao showed high transcript levels in the flowering stages compared to white-flowered buckwheat Tanno. In addition, cyanidin 3-*O*-glucoside and cyanidin 3-*O*-rutinoside contents of Gan-Chao were higher than those of Tanno. From these results, anthocyanin in the red-flowered buckwheat Gan-Chao flower has an accumulation mechanism different from that in Tanno flower. Moreover, elevated *FeANS* and *FeDFR* expression in seed stage 1 strongly suggested that these genes are associated with increased anthocyanin biosynthesis in seeds. Our results suggest that the synthesis and accumulation of specific anthocyanins in the red-flowered buckwheat Gan-Chao are regulated by genes involved in anthocyanin biosynthesis. The first component of the PLS-DA indicated that high amounts of phenolic, shikimic, and pyruvic acids were present in the red-flowered buckwheat. This suggests that metabolomics could assist in differentiating mechanisms that regulate the conversion from primary to secondary metabolism in plants. Metabolite correlation and network analysis showed the interdependencies with individual metabolites and metabolic pathways. Thus, the present study results could aid in clarifying anthocyanin biosynthesis in red-flowered buckwheat.

■ ASSOCIATED CONTENT

Ⓢ Supporting Information

Additional tables. This material is available free of charge via the Internet at http://pubs.acs.org.

■ AUTHOR INFORMATION

Corresponding Authors

*(J.K.K.) Mailing address: Division of Life Sciences, College of Life Sciences and Bioengineering, Incheon National University, Incheon 406-772, Republic of Korea. Phone: +82-32-835-8241. Fax: +82-32-835-0763. E-mail: kjkpj@incheon.ac.kr.

*(S.U.P.) Mailing address: Department of Crop Science, Chungnam National University, 99 Daehak-Ro, Yuseong-Gu, Daejeon 305-764, Republic of Korea. Phone: +82-42-821-5730. Fax: +82-42-822-2631. E-mail: supark@cnu.ac.kr

Funding

This work (K11101) was supported by the Korea Institute of Oriental Medicine (KIOM) grant funded by the Korea government and also partially from the Next-Generation

BioGreen 21 Program (SSAC, PJ009520), Rural Development Administration, Republic of Korea.

Notes

The authors declare no competing financial interest.

■ ABBREVIATIONS USED

HPLC, high-performance liquid chromatography; PAL, phenylalanine ammonia-lyase; C4H, cinnamate 4-hydroxylase; 4CL, 4-coumaroyl CoA ligase; CHS, chalcone synthase; CHI, chalcone isomerase; F3H, flavone 3-hydroxylase; FLS, flavonol synthase; F3′H, flavonoid 3′-hydroxylase; ANS/LDOX, anthocyanidin synthase/leucoanthocyanidin dioxygenase; DFR, dihydroflavonol-4 reductase; UFGT, UDP-flavonoid glucosyltransferase

■ REFERENCES

(1) Bonafaccia, G.; Marocchini, M.; Kreft, I. Composition and technological properties of the flour and bran from common and tartary buckwheat. *Food Chem.* **2003**, *80*, 9−15.

(2) Lin, R.; Tao, Y.; Li, X. Preliminary division of cultural and ecological regions of Chinese buckwheat. *Fagopyrum* **1992**, *12*, 48−55.

(3) Bonafaccia, G.; Galli, V.; Francisci, R.; Mair, V.; Škrabanja, V.; Kreft, I. Characteristics of spelt wheat products and nutritional value of spelt wheat-based bread. *Food Chem.* **2000**, *68*, 437−441.

(4) Takeuchi, K. A manufacturing process to produce buckwheat petals and seedling juice. Jpn. Patent 3771483, 2006.

(5) Kreft, S.; Strukelj, B.; Gaberscik, A.; Kreft, I. Rutin in buckwheat herbs grown at different UV-B radiation levels: comparison of two UV spectrophotometric and an HPLC method. *J. Exp. Bot.* **2002**, *53*, 1801−1804.

(6) Landberg, R.; Sun, Q.; Rimm, E. B.; Cassidy, A.; Scalbert, A.; Mantzoros, C. S.; Hu, F. B.; van Dam, R. M. Selected dietary flavonoids are associated with markers of inflammation and endothelial dysfunction in U.S. women. *J. Nutr.* **2011**, *141*, 618−625.

(7) Kuntić, V.; Filipović, I.; Vujić, Z. Effects of rutin and hesperidin and their Al(III) and Cu(II) complexes on in vitro plasma coagulation assays. *Molecules* **2011**, *16*, 1378−1388.

(8) Li, X.; Park, N. I.; Xu, H.; Woo, S. H.; Park, C. H.; Park, S. U. Differential expression of flavonoid biosynthesis genes and accumulation of phenolic compounds in common buckwheat (*Fagopyrum esculentum*). *J. Agric. Food Chem.* **2010**, *58*, 12176−12181.

(9) Winkel-Shirley, B. Flavonoid biosynthesis. A colorful model for genetics, biochemistry, cell biology, and biotechnology. *Plant Physiol.* **2001**, *126*, 485−493.

(10) Dixon, R.; Paiva, N. Stress-induced phenylpropanoid metabolism. *Plant Cell* **1995**, *7*, 1085−1097.

(11) Russel, D. W. The metabolism of aromatic compounds in higher plants. X. Properties of the cinnamic acid 4-hydroxylase of pea seedlings and some aspects of its metabolic and developmental control. *J. Biol. Chem.* **1971**, *246*, 3870−3878.

(12) Kristiansen, K. N.; Rohde, W. Structure of the *Hordeum vulgare* gene encoding dihydroflavonol-4-reductase and molecular analysis of ant18 mutants blocked in flavonoid synthesis. *Mol. Gen. Genet.* **1991**, *230*, 49−59.

(13) Martens, S.; Teeri, T.; Forkmann, G. Heterologous expression of dihydroflavonol 4-reductases from various plants. *FEBS Lett.* **2002**, *531*, 453−458.

(14) Strack, D.; Wray, V. *Methods in Plant Biochemistry*; Academic Press: London, UK, 1989; Vol. 1, pp 325−356.

(15) Park, N. I.; Xu, H.; Li, X.; Jang, I. H.; Park, S. H.; Ahn, G. H.; Lim, Y. P.; Kim, S. J.; Park, S. U. Anthocyanin accumulation and expression of anthocaynin biosynthetic genes in radish (*Raphanus sativus*). *J. Agric. Food Chem.* **2011**, *59*, 6034−6039.

(16) Jaakola, L.; Hohtola, A. Effect of latitude on flavonoid biosynthesis in plants. *Plant Cell Environ.* **2010**, *33*, 1239−1247.

(17) Hoekenga, O. A. Using metabolomics to estimate unintended effects in transgenic crop plants: problems, promises, and opportunities. *J. Biomol. Technol.* **2008**, *19*, 159−166.

(18) Kok, E. J.; Keijer, J.; Kleter, G. A.; Kuiper, H. A. Comparative safety assessment of plant-derived foods. *Reg. Toxicol. Pharmacol.* **2008**, *50*, 98−113.

(19) Kobayashi, S.; Nagasawa, S.; Yamamoto, Y.; Donghyo, K.; Bamba, T.; Fukusaki, E. Metabolic profiling and identification of the genetic varieties and agricultural origin of *Cnidium officinale* and *Ligusticum chuanxiong*. *J. Biosci. Bioeng.* **2012**, *114*, 86−91.

(20) Suzuki, T.; Kim, S. J.; Mohamed, Z. I. S.; Mukasa, Y.; Takigawa, S.; Matsuura-endo, C.; Yamauchi, H.; Hashimoto, N.; Noda, T.; Saito, T. Structural identification of anthocyanins and analysis of concentrations during growth and flowering in buckwheat (*Fagopyrum esculentum* Moench) Petals. *J. Agric. Food Chem.* **2007**, *55*, 9571−9575.

(21) Gambino, G.; Perrone, I.; Gribaudo, I. A rapid and effective method for RNA extraction from different tissues of grapevine and other woody plants. *Phytochem. Anal.* **2008**, *19*, 520−525.

(22) Li, X.; Thwe, A. A.; Park, N. I.; Suzuki, T.; Kim, S.-J.; Park, S. U. Accumulation of phenylpropanoids and correlated gene expression during the development of tatary buckwheat sprouts. *J. Agric. Food Chem.* **2012**, *60*, 5629−5635.

(23) Kim, J. K.; Park, S. Y.; Lee, S. M.; Lim, S. H.; Kim, H. J.; Oh, S. D.; Yeo, Y. S.; Cho, H. S.; Ha, S.-H. Unintended polar metabolite profiling of carotenoid-biofortified transgenic rice reveals substantial equivalence to its non-transgenic counterpart. *Plant Biotechnol. Rep.* **2013**, *7*, 121−128.

(24) Zhang, B.; Hu, Z.; Zhang, Y.; Li, Y.; Zhou, S.; Chen, G. A putative functional MYB transcription factor induced by low temperature regulates anthocyanin biosynthesis in purple kale (*Brassica oleracea* var. acephala f. tricolor). *Plant Cell Rep.* **2012**, *31*, 281−289.

(25) Martin, C.; Gerats, T. Control of pigment biosynthesis genes during petal development. *Plant Cell* **1993**, *5*, 1253−1264.

(26) Quattrocchio, F.; Baudry, A.; Lepiniec, L.; Grotewold, E. The regulation of flavonoid biosynthesis. In *The Science of Flavonoids*; Grotewold, E., Ed.; Springer: Berlin, Germany, 2006; pp 97−122.

(27) Park, N. I.; Li, X.; Suzuki, T.; Kim, S.-J.; Woo, S.-H.; Park, C. H.; Park, S. U. Differential expression of anthocyanin biosynthetic genes and anthocyanin accumulation in tartary buckwheat cultivars 'Hokkai T8' and 'Hokkai T10'. *J. Agric. Food Chem.* **2011**, *59*, 2356−2361.

(28) Povero, G.; Gonzali, S.; Bassolino, L.; Mazzucato, A.; Perata, P. Transcriptional analysis in high-anthocyanin tomatoes reveals synergistic effect of Aft and atv genes. *J. Plant Physiol.* **2011**, *168*, 270−279.

(29) Gerats, T.; Strommer, J. *Petunia: Evolutionary Developmental and Physiologycal Genetics*, 2nd ed.; Springer: Nijmegen, The Netherlands, 2009.

(30) Ferri, M.; Tassoni, A.; Franceschetti, M.; Righetti, L.; Naldrett, M. J.; Bagni, N. Chitosan treatment induces changes of protein expression profile and stilbene distribution in *Vitis vinifera* cell suspensions. *Proteomics* **2009**, *9*, 610−624.

(31) Inoue, K.; Hosokama, Y.; Shimadate, T. Anthocyanin pigments of buckwheat hypocotyls. *Kenkyu Kiyo Nihon Daigaku Bunrigakubu Shizen Kagaku Kenkyusho* **1982**, *17*, 26.

(32) Troyer, J. R. Anthocyanin pigments of buckwheat hypocotyls. *Ohio J. Sci.* **1982**, *58*, 187.

(33) Troyer, J. R. Anthocyanin formation in excised segments of buckwheat seedling hypocotyls. *Plant Physiol.* **1964**, *39*, 907.

(34) Prior, R. L.; Lazarus, S. A.; Cao, G.; Muccitelli, H.; Hammerstone, J. F. Identification of procyanidins and anthocyanins in blueberries and cranberries (*Vaccinium* spp.) using hig-performance liquid chromatography/mass spectrometry. *J. Agric. Food Chem.* **2001**, *49*, 1270−1276.

(35) Dugo, P.; Mondello, L.; Morabito, D.; Dugo, G. Characterization of the anthocyanin fraction of Sicilian blood orange juice by micro-HPLC-ESI/MS. *J. Agric. Food Chem.* **2003**, *51*, 1173−1176.

(36) Choung, M.-G.; Baek, I.-Y.; Kang, S.-T.; Han, W.-Y.; Shin, D.-C.; Moon, H.-P.; Kang, K.-H. Isolation and determination of anthocyanins in seed coats of black soybean (*Glycine max* (L.) Merr.). *J. Agric. Food Chem.* **2001**, *49*, 5848−5851.

(37) Thwe, A. A.; Kim, J. K.; Li, X.; Kim, Y. B.; Uddin, M. R.; Kim, S. J.; Suzuki, T.; Park, N. I.; Park, S. U. Metabolomic analysis and phenylpropanoid biosynthesis in hairy root culture of tartary buckwheat cultivars. *PLoS One* **2013**, *8*, e65349.
(38) Kim, Y. B.; Kim, J. K.; Xu, H.; Park, W. T.; Tuan, P. A.; Li, X.; Chung, E.; Lee, J.-H.; Park, S. U. Metabolomics analysis and biosynthesis of rosmarinic acid from *Agastache rugosa* Kuntze treated with methyl jasmonate. *PLoS One* **2013**, *8*, e64199.